

# Optimal sail angle computation for an autonomous sailboat robot

Hadi Saoud<sup>1</sup>, Minh-Duc Hua<sup>1</sup>, Frederic Plumet<sup>1</sup> and Faiz Ben Amar<sup>1</sup>

Institute for Intelligent Systems and Robotics (ISIR)

UPMC Univ Paris 06, CNRS - UMR 7222, 75005 Paris - France

**Abstract**—A method to compute the optimal sail angle for an autonomous sailboat is proposed, which allows for maximizing the longitudinal velocity while maintaining safe sailing conditions by limiting the roll angle. A simplified 4-DOF dynamic model of the sailboat is used to obtain the roll dynamics and longitudinal sail force. From these expressions, we derive a cost function which depends on the thrust force. The cost needs to be minimized under stability constraint in roll motion while the system is subject to a bound on the roll angle. Numerical simulations, using a full nonlinear dynamic model of the sailboat, show the improved performance of the proposed method, compared to traditional solutions that can be found in the literature.

## I. INTRODUCTION

Due to their low energy consumption, autonomous sailing robots provide a promising solution for long-term observation or monitoring missions in the oceans and a lot of sailing robot projects were launched worldwide during the last decade [1]–[8]. The control of an autonomous sailboat (i.e. controlling its heading while ensuring a “good” trimming of the sails) is challenging since the thrust force depends on uncontrollable and partially unpredictable wind. Moreover, such vehicles exhibit complex behaviour due to aero- and hydrodynamic properties of their sails and hull.

The problem of planning and controlling the heading angle of an autonomous sailboat has been widely studied (see [1], [3], [8]–[11] among others), but little attention has been paid to the computation of the sail angle. On manned sailboats, sail trimming is mainly carried out on the basis of the experience and skills of the sailors. Sailors can also use VPP programs to correct their sailing configurations (VPP are commercial products that give the theoretical maximum velocity of a sailboat for each wind condition [12]). Sailors’ skills and experience have been adapted to the case of autonomous sailboats using either a linear relationship between the sail’s angle of attack and the sail angle (including or not saturation and hysteresis [3], [13]) or by using fuzzy logic controller [14] [15]. None of these methods is focused on the computation of a sail angle to maximize the longitudinal speed (surge) of a sailboat. Some other methods have been proposed like the extremum-seeking [16] for the on-line speed optimization when sail model is unknown. Such method usually has a long convergence time which could be annoying with fast varying wind conditions [17].

Obviously, maximizing the speed of a sailboat is important not only for racing purpose but also to be consistent with

mission objectives for example. Maximizing the speed of a sailboat also improves the manoeuvrability and the stability of the heading controller since the torque produced by the rudder depends on the square of the velocity of the fluid. On the other side, when the speed of a sailboat increases, the forces acting on the sail may increase the heeling (or roll) angle and thus the risk of capsizing.

In this paper, we present a method for calculating an optimal sailing angle that maximizes the speed of a sailboat while ensuring that the heeling angle remains bounded by a pre-defined value. This method is based on the study of the steady state behaviour in surge and roll and is formulated as an optimization problem (thrust force) subject to equality constraint (roll stability). A major contribution of this paper is to demonstrate that the choice of such an optimal sailing angle mathematically limits the steady heeling angle to a value smaller than  $\pi/4$  radians. Moreover, other values for the maximum steady heeling angle (less than  $\pi/4$  radians) can be easily introduced in the optimization process in order to better reflect sailboat stability limits.

In this study, we assume that the sailboat has only one mainsail with well known lift and drag coefficients and that there is no aerodynamic interaction between the sail and the rest of the sailboat.

The paper is organized as follow: we first describe a 4 DOF dynamic model of a sailboat and, under some assumptions, derive the expression of the longitudinal sail force and equilibrium equation between the sail torque and restoring torque. Then, we formulate the computation of the optimal sail angle as a minimization problem subject to equality constraint on the roll stability, first without limiting the roll angle (section VI-A) and then including a saturation of the roll angle (section VI-B). A numerical study for a real sail is presented in the last section. Numerical simulations, based on the full nonlinear dynamic model of a sailboat, show the performance of this optimal sail computation, compared to other methods described in the literature.

## II. NOTATION

- $\{e_1, e_2, e_3\}$  denotes the canonical basis of  $\mathbb{R}^3$ .
- For any  $x \in \mathbb{R}^3$ , the notation  $x_{\times}$  denotes the skew-symmetric matrix associated with  $x$ , i.e.  $x_{\times}y = x \times y$ ,  $\forall y \in \mathbb{R}^3$ .
- For any affine vector  $\vec{x}$ ,  $x^{\mathcal{X}}$  denotes the vector of coordinates of  $\vec{x}$  in the basis of the frame  $\mathcal{X}$ .

<sup>1</sup>All authors, E-mails: lastname@isir.upmc.fr

- $R_{v,\theta} \in SO(3)$  denotes the rotation matrix that rotate a vector by an angle  $\theta$  around  $v$ .
- $G$ : sailboat center of mass (CoM).
- $G_s$ : center of pressure of the sail (assumed to be fixed).
- $\mathcal{I} = \{0; \vec{i}_0, \vec{j}_0, \vec{k}_0\}$ : inertial frame chosen as the North-West-Up frame.
- $\mathcal{B} = \{G; \vec{i}, \vec{j}, \vec{k}\}$ : body frame fixed to the hull.
- $\mathcal{S} = \{G_s; \vec{i}_s, \vec{j}_s, \vec{k}_s\}$ : sail-fixed frame.
- $M \in \mathbb{R}^{3 \times 3}$ ,  $J = \text{diag}([J_{11} J_{22} J_{33}]) \in \mathbb{R}^{3 \times 3}$ : sailboat's mass and inertia matrices, including real-body and added-mass components.
- $\vec{x}$ ,  $\vec{x}_s$ : position of  $G$  and  $G_s$  w.r.t. the inertial frame.
- $\vec{\omega}$ : angular velocity of the body-fixed frame w.r.t. the inertial frame.
- $\vec{v}$ : linear velocity of  $G$  w.r.t. the inertial frame.
- $\vec{v}_s$ : linear velocity of  $G_s$  w.r.t. the inertial frame.
- $\vec{v}_w$ : wind velocity w.r.t. the inertial frame.
- $\vec{v}_{as}$ : apparent velocity of the sail.
- $x, R, \omega, v$ : short notation of  $x^{\mathcal{I}}, R_{\mathcal{B}}^{\mathcal{I}}, \omega^{\mathcal{B}}, v^{\mathcal{B}}$ .
- $\delta_s, \alpha_s$ : sail angle and sail angle of attack.
- $C_s^L(\cdot), C_s^D(\cdot)$ : lift and drag coefficients of the sail.
- $\nabla f(x) = \frac{\partial f}{\partial x}$
- $\phi, \psi$ : roll and yaw angles of the sailboat.
- $c(\cdot) \triangleq \cos(\cdot)$  and  $s(\cdot) \triangleq \sin(\cdot)$
- $h_s := GG_s \cdot \vec{k}_s$ : vertical distance between  $G$  and  $G_s$
- $V_{long}, V_{lat}$ : longitudinal and lateral velocity of the sailboat
- $\sum \vec{F}, \sum \vec{\tau}$ : sum of forces and torques applied on  $G$
- $l_\phi$ : metacentric height of the sailboat
- $\Theta_V$ : angle of apparent wind speed w.r.t the body frame

### III. MODEL USED

The 6-DOF model used for the sailboat is a classical model in marine robotics [10], [18]. The dynamic can be summarized as follows:

$$\begin{cases} M\dot{v} = -\omega \times Mv + \sum F^{\mathcal{B}} \\ J\dot{\omega} = -\omega \times J\omega + \sum \tau^{\mathcal{B}} \end{cases} \quad (1)$$

with  $v = [v_1, v_2, v_3]^{\top}$  and  $\omega = [\omega_1, \omega_2, \omega_3]^{\top}$ .

By approximating the hull to a volume with three mutually perpendicular axes of symmetry, the contributions of the off-diagonal elements in the added mass matrix can be neglected, i.e. both mass and inertia matrices are diagonal.

**Assumption 1** *The pitch motion and vertical motion are small so that we can use a 4 DOF dynamic model:  $x, y$  translations and roll, yaw ( $\phi, \psi$ ) rotations.*

Thus, kinematic equations of motion are given by:

$$\dot{\phi} = \omega_1, \quad \dot{\psi} = \omega_3 (\cos \phi)^{-1}$$

The longitudinal and lateral velocities  $V_{long}, V_{lat}$  of the sailboat are defined as:

$$\begin{bmatrix} V_{long} \\ V_{lat} \\ 0 \end{bmatrix} := R_{z,\psi}^{\top} \dot{x} = R_{x,\phi} v$$

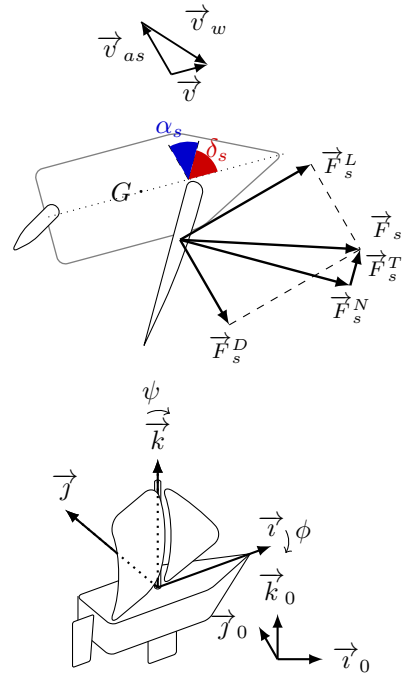


Fig. 1: Frames orientation and wind efforts

From here, roll dynamic can be expressed as the following:

$$\begin{aligned} \ddot{\phi} = \dot{\omega}_1 &= -e_1^{\top} J^{-1} \omega \times J \omega + e_1^{\top} J^{-1} \sum \tau^{\mathcal{B}} \\ &= \frac{-J_{22} + J_{33}}{J_{11}} \omega_3^2 \tan \phi - \frac{e_1^{\top}}{J_{11}} \sum \tau^{\mathcal{B}} \end{aligned}$$

Assuming that roll dynamic is much faster than yaw dynamic ( $\phi \gg \psi$ ), the last one can be neglected leading to the following expression:

$$\ddot{\phi} = -\frac{e_1^{\top}}{J_{11}} \sum \tau^{\mathcal{B}}$$

This dynamic equation will be used later in the expression of the equilibrium constraint of the sailboat.

### IV. PROBLEM FORMULATION

By neglecting the angular velocity of the rotating sail, the apparent velocity of the sail w.r.t the surrounding air  $\vec{v}_{as}$  is defined by:

$$\vec{v}_{as} = \vec{v} - \vec{v}_w$$

Let's define  $V$  as the result of rotating  $v_{as}^{\mathcal{I}}$  around the  $\vec{k}_0$  axis:

$$V \triangleq \begin{bmatrix} V_1 \\ V_2 \\ 0 \end{bmatrix} = R_{z,\psi}^{\top} v_{as}^{\mathcal{I}} = \begin{bmatrix} V_{long} \\ V_{lat} \\ 0 \end{bmatrix} - R_{z,\psi}^{\top} v_w^{\mathcal{I}}$$

Then, the angle of apparent wind speed w.r.t the body frame is given by:

$$\Theta_V \triangleq \text{atan2}(V_2, V_1)$$

Note that,  $\Theta_V$  is related to the apparent wind angle (AWA) measured by on-board anemometer by:

$$\tan(\text{AWA}) = \cos \phi \tan \Theta_V$$

The angle of attack  $\alpha_s$  can be defined as [10]:

$$\sin \alpha_s = \frac{-v_{as,2}^S}{|\vec{v}_{as}|}$$

with

$$v_{as,2}^S = -V_1 \sin \delta_s + V_2 \cos \phi \cos \delta_s$$

$$|\vec{v}_{as}| = |V| = \sqrt{V_1^2 + V_2^2}$$

To simplify the problem, we did several assumptions:

**Assumption 2** *The wind velocity is assumed to be always parallel to the water surface, which is also assumed to be flat.*

**Assumption 3** *Amplitude of apparent speed is non-null ( $|V| > 0$ ) for all time.*

Usually, to describe efforts on sail, we use lift and drag coefficients [19] related to the forces generated by the apparent wind in both apparent wind direction and normal to the apparent wind direction. By using these coefficients, effort on the sail  $\vec{F}_s$  is given by [10]:

$$\vec{F}_s = -\lambda_s (C_s^D(\alpha_s) - C_s^L(\alpha_s) \tan \alpha_s) |\vec{v}_{as}| \vec{v}_{as}$$

$$+ \lambda_s \frac{C_s^L(\alpha_s)}{\cos \alpha_s} |\vec{v}_{as}|^2 \vec{j}_s$$

with  $\lambda_s = \frac{1}{2} \rho_{air} S_s$  ( $\rho_{air}$ : air density,  $S_s$ : surface of the sail).

The effort  $\vec{F}_s$  can be written as the sum of two terms: one normal to the sail plan (parallel to  $\vec{j}_s$ ) and one tangential to the sail (parallel to  $\vec{v}_s$ ). This lead us to compute a normal coefficient  $C_s^N$  and a tangential coefficient  $C_s^T$ :

$$C_s^T(\alpha_s) := C_s^L(\alpha_s) \sin \alpha_s - C_s^D(\alpha_s) \cos \alpha_s$$

$$C_s^N(\alpha_s) := C_s^L(\alpha_s) \cos \alpha_s + C_s^D(\alpha_s) \sin \alpha_s$$

The sail force can now be written as the following:

$$\vec{F}_s = +\lambda_s C_s^N(\alpha_s) |V|^2 \vec{j}_s - \lambda_s C_s^T(\alpha_s) |V|^2 \vec{v}_s$$

From curves presented in [19], we noticed that  $C_s^T \ll C_s^N$  on sails that respect the following conditions: 1) high aspect ratio ( $AR > 4$ ), 2) low camber ( $c < \frac{1}{15}$ ).

Furthermore, one can note that the normal coefficient  $C_s^N(\alpha_s)$  of these kind of sails is a monotonically increasing function of  $\sin \alpha_s$ .

**Assumption 4** *The tangential component is assumed to be very small with respect to the normal component so that we can neglect the tangential force:*

$$\vec{F}_s \approx -\lambda_s C_s^N(\alpha_s) |V|^2 \vec{j}_s$$

This assumption is verified in almost all sails described in [19].

**Assumption 5** *The sail is fully actuated so that the sail angle can take any value, without constraint related to apparent wind direction, i.e.  $\delta_s \in [-\pi, \pi] \forall \Theta_V$ .*

The roll sail torque and the longitudinal sail force are given by:

$$\begin{cases} \tau_{s,1}^B = -\lambda_s h_s C_s^N(\alpha_s) |V|^2 \cos \delta_s \\ F_{s,1}^B = -\lambda_s C_s^N(\alpha_s) |V|^2 \sin \delta_s \end{cases}$$

Our idea is to write  $C_s^N(\alpha_s)$  as a function of  $\sin \alpha_s$ :

$$C_s^N(\alpha_s) = f(\sin \alpha_s)$$

where  $f(\cdot) : [-1, 1] \rightarrow \mathbb{R}$  is a differentiable odd function satisfying the following properties:

$$\begin{aligned} \text{sign}(f(x)) &= \text{sign}(x) \quad , f(x) = 0 \text{ iff } x = 0 \\ f(-x) &= -f(x) \quad , \nabla f(x) = \nabla f(-x) \end{aligned} \quad (2)$$

Thus, the roll sail torque and the longitudinal sail force can be rewritten as:

$$\begin{cases} \tau_{s,1} &= -\lambda_s h_s f(\sin \alpha_s) |V|^2 \cos \delta_s \\ F_{s,1} &= -\lambda_s f(\sin \alpha_s) |V|^2 \sin \delta_s \end{cases} \quad (3)$$

We also assume that, at roll equilibrium, torque effects from rudder, keel and hydrodynamic efforts are neglected due to the sailboat's structure. The remaining sail torque  $\tau_s^B$  and restoring torque  $\tau_{res}^B$  give the equilibrium condition in roll motion:

$$0 = \ddot{\phi} = \tau_{rep,1}^B + \tau_{s,1}^B$$

$$= -mgl_\phi \sin \phi - \lambda_s h_s f(\sin \alpha_s) |V|^2 \cos \delta_s \quad (4)$$

## V. OPTIMAL SAIL ANGLE DETERMINATION

Since we want to maximize the longitudinal velocity, we try to maximize the sail force  $F_{s,1} = -\lambda_s f(\sin \alpha_s) |V|^2 \sin \delta_s$  under the equilibrium condition in roll motion to avoid capsizing. This can be formulated as a minimization problem subject to an equality constraint:

$$\begin{aligned} \min \quad & \mathcal{J}(\delta_s, \phi) := f(\sin \alpha_s) \sin \delta_s \\ \text{s.t.} \quad & \beta \sin \phi + f(\sin \alpha_s) \cos \delta_s = 0 \end{aligned} \quad (5)$$

with

$$\sin \alpha_s = \bar{V}_1 \sin \delta_s - \bar{V}_2 \cos \phi \cos \delta_s$$

$$\bar{V}_{1,2} := \frac{V_{1,2}}{|V|} \quad \& \quad \beta := \frac{mgl_\phi}{\lambda_s h_s |V|^2}$$

To take into account the equilibrium constraint in the minimization problem, we compute the Lagrangian:

$$\mathcal{L} = f(\sin \alpha_s) \sin \delta_s + \lambda (\beta \sin \phi + f(\sin \alpha_s) \cos \delta_s)$$

Finding the optimal values  $\delta_s^*$  and  $\phi^*$  can be done by finding the minima of  $\mathcal{L}$  through computing its partial derivative and solving (6) simultaneously. The global minimum is the solution of (6) that leads to a minimal value of the cost function.

$$\begin{cases} 0 = \frac{\partial \mathcal{L}}{\partial \lambda} = \beta \sin \phi + f(\sin \alpha_s) \cos \delta_s \\ 0 = \frac{\partial \mathcal{L}}{\partial \phi} = \nabla f(\sin \alpha_s) (\bar{V}_2 \sin \phi \cos \delta_s) \sin \delta_s \\ \quad + \lambda [\beta \cos \phi + \nabla f(\sin \alpha_s) (\bar{V}_2 \sin \phi \cos \delta_s) \cos \delta_s] \\ 0 = \frac{\partial \mathcal{L}}{\partial \delta_s} = \nabla f(\sin \alpha_s) (\bar{V}_1 \cos \delta_s + \bar{V}_2 \cos \phi \sin \delta_s) \sin \delta_s + f(\sin \alpha_s) \cos \delta_s \\ \quad + \lambda [\nabla f(\sin \alpha_s) (\bar{V}_1 \cos \delta_s + \bar{V}_2 \cos \phi \sin \delta_s) \cos \delta_s - f(\sin \alpha_s) \sin \delta_s] \end{cases} \quad (6)$$

One deduces from  $0 = \frac{\partial \mathcal{L}}{\partial \delta_s}$  that:

$$\lambda = \frac{-\nabla f (\bar{V}_1 \cos \delta_s + \bar{V}_2 \cos \phi \sin \delta_s) \sin \delta_s - f \cos \delta_s}{\nabla f (\bar{V}_1 \cos \delta_s + \bar{V}_2 \cos \phi \sin \delta_s) \cos \delta_s - f \sin \delta_s}$$

Replacing  $\lambda$  into the expression  $0 = \frac{\partial \mathcal{L}}{\partial \phi}$  one obtains:

$$f \nabla f (\bar{V}_2 s \phi c \delta_s) + \beta c \phi [\nabla f (\bar{V}_1 c \delta_s + \bar{V}_2 c \phi s \delta_s) s \delta_s + f c \delta_s] = 0$$

Replacing  $\cos \delta_s = -(\beta/f) \sin \phi$  and  $\bar{V}_1 \sin \delta_s = \sin \alpha_s + \bar{V}_2 \cos \phi \cos \delta_s$  into the above equation, we get:

$$-\beta \nabla f \bar{V}_2 s^2 \phi + \beta c \phi [\nabla f (\bar{V}_1 c \delta_s + \bar{V}_2 \cos \phi s \delta_s) s \delta_s + f c \delta_s] = 0$$

that lead to a relation between the roll angle  $\phi$  and the angle of attack  $\alpha_s$ :

$$\tan(2\phi) = \frac{2\bar{V}_2}{\beta} \left( \frac{f \nabla f}{\sin \alpha_s \nabla f + f} \right) \quad (7)$$

In summary, instead of solving (6), the following equations need to be solved in order to find the minima:

$$\begin{cases} \sin \alpha_s = \bar{V}_1 \sin \delta_s - \bar{V}_2 \cos \phi \cos \delta_s & (8a) \\ \beta \sin \phi + f \cos \delta_s = 0 & (8b) \end{cases}$$

$$\begin{cases} \tan(2\phi) = \frac{2\bar{V}_2}{\beta} \left( \frac{f \nabla f}{\sin \alpha_s \nabla f + f} \right) & (8c) \end{cases}$$

**Remark 1** Relation (8c) implies that the optimal roll angle  $\phi^*$  is bounded by  $\pi/4$ , i.e.  $|\phi^*| \leq \pi/4$ . Moreover, in the case where  $f$  is an increasing function, one ensures that

$$\text{sign}(\phi^*) = \text{sign}(\bar{V}_2)$$

Indeed, since  $\nabla f$  is positive as  $f$  is an increasing function, and since  $f(\sin \alpha_s)$  has the same sign as  $\sin \alpha_s$ , one verifies that  $\frac{f \nabla f}{\sin \alpha_s \nabla f + f}$  is positive. Thus,  $\text{sign}(\phi^*) = \text{sign}(\tan(2\phi^*)) = \text{sign}(\bar{V}_2)$ .

**Lemma 1** If  $(\delta_s^*, \phi^*)$  is the optimal solution to the minimization problem (5), then  $(\delta_s^* \pm \pi, \phi^*)$  is also an optimal solution to (5).

**Proof:** Let  $\alpha_s^*$  such that  $\sin \alpha_s^* = \bar{V}_1 \sin \delta_s^* - \bar{V}_2 \cos \phi^* \cos \delta_s^*$ . Since  $(\delta_s^*, \phi^*, \alpha_s^*)$  is the optimal solution to (5), they satisfy (8). Therefore, we only need to show that  $(\delta_s^* \pm \pi, \phi^*, \alpha_s^* \pm \pi)$  also satisfy (8) and the associated cost function  $\mathcal{J}(\delta_s^* \pm \pi, \phi^*)$  is equal to the cost function induced by the optimal solution  $(\delta_s^*, \phi^*)$ , i.e.  $\mathcal{J}(\delta_s^* \pm \pi, \phi^*) = \mathcal{J}(\delta_s^*, \phi^*)$ . Indeed, relation (8a) with  $(\delta_s, \phi, \alpha_s) = (\delta_s^* \pm \pi, \phi^*, \alpha_s^* \pm \pi)$  writes

$$\begin{aligned} \sin(\alpha_s^* \pm \pi) &= \bar{V}_1 \sin(\delta_s^* \pm \pi) - \bar{V}_2 \cos \phi^* \cos(\delta_s^* \pm \pi) \\ \Leftrightarrow \sin \alpha_s^* &= \bar{V}_1 \sin \delta_s^* - \bar{V}_2 \cos \phi^* \cos \delta_s^* \end{aligned}$$

which is exactly relation (8a) with  $(\delta_s, \phi, \alpha_s) = (\delta_s^*, \phi^*, \alpha_s^*)$ . Similarly, using the fact that  $f(\cdot)$  is an odd function, one easily verifies that relations (8b) and (8c) also hold with  $(\delta_s, \phi, \alpha_s) = (\delta_s^* \pm \pi, \phi^*, \alpha_s^* \pm \pi)$ , provided that they are satisfied with  $(\delta_s, \phi, \alpha_s) = (\delta_s^*, \phi^*, \alpha_s^*)$ . It is also straightforward that  $\mathcal{J}(\delta_s^* \pm \pi, \phi^*) = \mathcal{J}(\delta_s^*, \phi^*)$ . ■

**Remark 2** As a result of lemma 1, if the sail angle is physically limited to the interval  $[-\pi/2, \pi/2]$ , there exists always one solution inside this interval.

## VI. SOLVING THE OPTIMAL SAIL PROBLEM

### A. Without saturation on optimal Roll angle

System of equations (8) need to be solved in real-time on the sailboat to continuously get an optimal sail angle reference. Because this computation can be time-consuming, we transform the system to get a single nonlinear equation with a single variable.

Denote:

$$\begin{cases} x := \sin \alpha_s & \in [-1, 1] \\ y := \sin(2\phi) & \in ]-1, 1[ \\ z := \sin \delta_s & \in [-1, 1] \end{cases} \quad (9)$$

The cost function is then:  $\mathcal{J}(x, z) = f(x)z$

From (8a) and (8b) one deduces:

$$\sin \alpha_s = \bar{V}_1 \sin \delta_s + \frac{\bar{V}_2 \beta \sin(2\phi)}{2f} \implies$$

$$x = \bar{V}_1 z + \frac{\bar{V}_2 \beta}{2} \frac{y}{f(x)}$$

From here and by using (8) and (9), one obtains the following equations:

$$\begin{cases} x = \bar{V}_1 z + \frac{\bar{V}_2 \beta}{2} \frac{y}{f(x)} & (10a) \end{cases}$$

$$\begin{cases} \frac{\beta}{\sqrt{2}} \frac{y}{f(x)} = \mp \sqrt{1 - z^2} \sqrt{\sqrt{1 - y^2} + 1} & (10b) \end{cases}$$

$$\begin{cases} \frac{y}{\sqrt{1 - y^2}} = \frac{2\bar{V}_2}{\beta} \frac{f(x) \nabla f(x)}{x \nabla f(x) + f(x)} & (10c) \end{cases}$$

for  $x \in [-1, 1]$ ,  $y \in ]-1, 1[$ ,  $z \in [-1, 1]$ .

Letting:

$$g(x) := \frac{f(x) \nabla f(x)}{x \nabla f(x) + f(x)} > 0$$

$$\bar{g}(x) := \frac{2\bar{V}_2}{\beta} g(x) = \frac{2\lambda_s h_s |V| V_2}{m g l_\phi} g(x)$$

one deduces from (10c):

$$y = \frac{\bar{g}(x)}{\sqrt{1 + \bar{g}^2(x)}}, \quad \sqrt{1 - y^2} = \frac{1}{\sqrt{1 + \bar{g}^2(x)}}$$

and, thus, from (10b):

$$\sqrt{1 - z^2} = \frac{\mp \beta \bar{g}(x)}{\sqrt{2} f(x) (1 + \bar{g}^2(x))^{\frac{1}{4}} (1 + \sqrt{1 + \bar{g}^2(x)})^{\frac{1}{2}}} \quad (11)$$

One deduces from (10a):

$$z = \frac{1}{\bar{V}_1} \left[ x - \bar{V}_2^2 \frac{g(x)}{f(x) \sqrt{1 + \bar{g}^2(x)}} \right] \quad (12)$$

Using  $\bar{V}_1^2 z^2 + \bar{V}_1^2 (\sqrt{1 - z^2})^2 = \bar{V}_1^2$ , one finally gets the single nonlinear equation to be solved:

$$\begin{aligned} &2 \left[ x f(x) \sqrt{1 + \bar{g}^2(x)} - \bar{V}_2^2 g(x) \right]^2 + \\ &\frac{\bar{V}_1^2 \beta^2 \bar{g}^2(x) \sqrt{1 + \bar{g}^2(x)}}{1 + \sqrt{1 + \bar{g}^2(x)}} - 2\bar{V}_1^2 f^2(x) (1 + \bar{g}^2(x)) = 0 \end{aligned} \quad (13)$$

Solving the nonlinear equation (13) get the same results than solving the nonlinear system (8). The results are the local minima and maxima of the cost function. To find the global minimum, we can continue to evaluate the cost function for each value of  $x$ , in order to obtain the optimal value for  $x$  (and  $y$  and  $z$  accordingly).

**Lemma 2** *If  $x \in [-1, 1]$  is a solution to Eq. (13), then  $-x \in [-1, 1]$  is also a solution to Eq. (13).*

This lemma is a direct consequence of Lemma 1. It can also be easily proven using the properties (2) of  $f(\cdot)$ .

Solving Eq. (13) takes only few milliseconds on an Arm Cortex-A9 @ 1 Ghz and thus can be easily done on-line to continuously compute optimal sail angle  $\delta_s^*$ .

### B. Including saturation on Roll angle

Limiting roll angle may be a prime concern to avoid capsizing. If we want to limit the optimal roll angle such that  $|\phi^*| \leq \phi^{\max}$ , with  $\phi^{\max} < \pi/4$ , we can formulate the following minimization problem:

$$\begin{aligned} \min \quad & \mathcal{J}(\delta_s, \phi) := f(\sin \alpha_s) \sin \delta_s \\ \text{s.t. :} \quad & 1) \quad \beta \sin \phi + f(\sin \alpha_s) \cos \delta_s = 0 \\ & 2) \quad |\phi^*| \leq \phi^{\max} \end{aligned} \quad (14)$$

This is an optimization problem in a compact set. Therefore, a straightforward way to solve (13) is to compute a set  $\Lambda$  that include all potential solutions of (5). To take into account roll limit  $\phi^{\max}$ , the solution  $\phi = \text{sign}(\bar{V}_2)\phi^{\max}$  must be added to  $\Lambda$ . The corresponding values of  $\alpha_s$  and  $\delta_s$  are obtained by solving numerically the roll motion equilibrium in 5 and  $\sin \alpha_s = \bar{V}_1 \sin \delta_s - \bar{V}_2 \cos \phi \cos \delta_s$ . By evaluating the cost of all potential solution in  $\Lambda$  and excluding solutions where  $|\phi| < \phi^{\max}$ , we can extract the optimal sail angle  $\delta_s^*$  so that equilibrium constraint is satisfied and  $|\phi| < \phi^{\max}$ .

## VII. NUMERICAL ANALYSIS AND SIMULATION

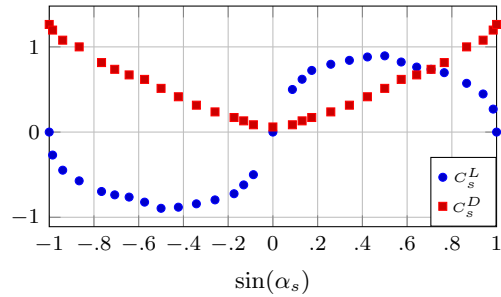
### A. Numerical case study for a flat sail

Let us consider a sail with no camber and  $AR = 5$  [19, p. 86]. The experimental data for the coefficients  $C_s^L$  and  $C_s^D$  are depicted in Fig. 2a. Fig. 2b shows the computed coefficients  $C_s^N$  and  $C_s^T$  versus the sine of the angle of attack (i.e.  $\sin \alpha_s$ ). It can be observed that the tangential component  $C_s^T$  evolves near zero and is largely dominated by the normal component  $C_s^N$ . Thus, Assumption 4 holds with good accuracy. An approximation by a polynomial of degree 5 for  $C_s^N$ , (red curve in Fig. 2b), is given by:

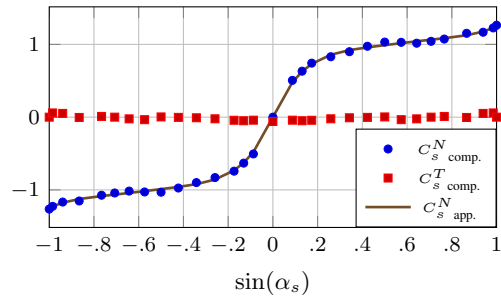
$$C_s^N(x) = \begin{cases} p_5 x^5 + p_4 x^4 + p_3 x^3 + p_2 x^2 + p_1 x & \text{if } x \geq 0 \\ p_5 x^5 - p_4 x^4 + p_3 x^3 - p_2 x^2 + p_1 x & \text{if } x < 0 \end{cases}$$

where  $x = \sin(\alpha_s)$  and with  $p_5 = 11.52$ ,  $p_4 = -33.79$ ,  $p_3 = 39.45$ ,  $p_2 = -23.07$  and  $p_1 = 7.15$ .

The numerical study used parameters defined in table I and have been done for two values of apparent velocity ( $|V| = 5$  and  $|V| = 8$ ) and two values of metacentric height ( $l_\phi = 0.1$  and  $l_\phi = 1$ ).



(a) Value of  $C_s^L$  and  $C_s^D$  v.s. sinus of the attack angle  $\alpha_s$  (from [19, p. 86]).



(b) Computed and approximated  $C_s^N$  and computed  $C_s^T$  v.s. sinus of the attack angle  $\alpha_s$ .

Fig. 2: Lift, drag, normal and tangential coefficients for a no camber sail with  $AR = 5$

TABLE I: Numerical values of the parameters

name	$m$	$S_s$	$g$	$\rho_{air}$	$h_s$
value	15	1	9.81	1.225	0.8

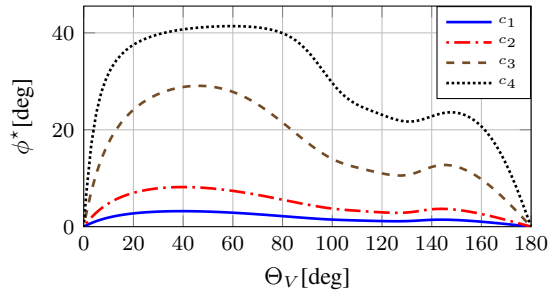
For this numerical study, equation (13) is solved numerically using, for instance, the Secant method. It exists normally 2 opposite-sign pairs of solutions for  $x$ , but we know that the sign of  $x$  should be opposite to that of  $\bar{V}_2$ . Therefore, for each  $\Theta_V$ , we have solved twice Eq. (13) with initial guesses, respectively, close to zero and  $\pm 1$  (depending on the sign of  $\bar{V}_2$ ). The comparison of the two resulting values of the cost function allows us the find the optimal solution.

We first consider the case where the roll angle is not limited and plot only the solutions where  $\delta_s \in [-\pi/2, \pi/2]$ .

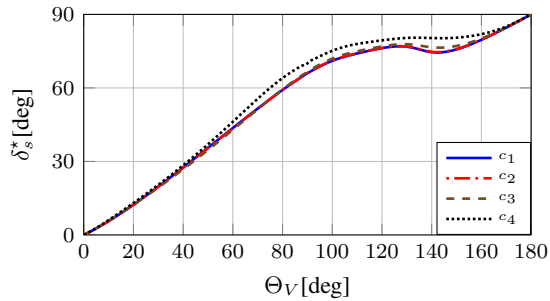
From 3b, we can note that, when wind speed is low, the relation between  $\delta_s$  and  $\Theta_V$  can be approximated by a linear function (as in [13]). In case of high wind speed, the curve begin to be saturated.

Now, we introduce the limitation to the roll angle, as in section VI-B. Figs. 4 show the effect of such limitation on  $\phi^*$  and  $\delta_s^*$ . We observe from 4a that a small variation in  $\delta_s$  lead to an important variation in  $\phi$ . We also notice that the main influence of limiting the roll angle is on the slope of the curve on its center part (when  $\delta_s \in [-\pi/2, \pi/2]$ ), i.e. when sailing upwind.

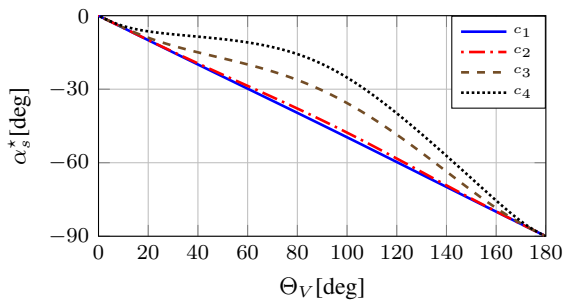
Figs 3 and 4 have origin symmetry. We observe from Fig 3c that angle of attack is not constant. In other words,



(a) Optimal roll angle  $\phi^*$  v.s. apparent wind angle  $\Theta_V$



(b) Optimal sail angle  $\delta_s^*$  v.s. apparent wind angle  $\Theta_V$



(c) Optimal angle of attack  $\alpha_s^*$  v.s. apparent wind angle  $\Theta_V$

Fig. 3: Optimal angles v.s. relative wind angle  $\Theta_V$  without limitation on  $\phi$  ( $c_1$ :  $|V| = 5$  &  $l_\phi = 1$ ,  $c_2$ :  $|V| = 8$  &  $l_\phi = 1$ ,  $c_3$ :  $|V| = 5$  &  $l_\phi = 0.1$ ,  $c_4$ :  $|V| = 8$  &  $l_\phi = 0.1$ ).

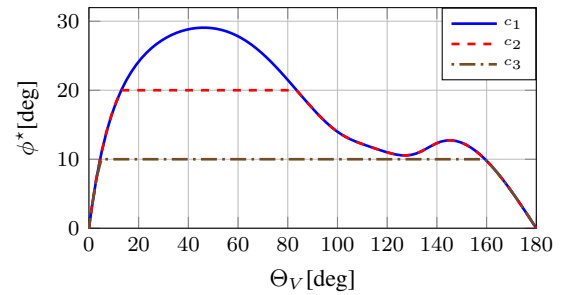
maintaining a constant angle of attack is not an optimal method for sail trimming.

### B. Simulation

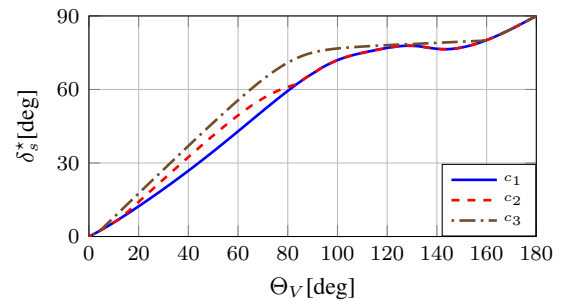
In order to evaluate the performance of this optimal sail selection, we perform numerical simulation and compare the results with the sail trimming method used in [3].

The sail trimming method used in [3] is summarized on Fig. 5: the sail angle is limited to  $\pm\pi/2$  when  $|\Theta_V| > 5\pi/6$  to save energy by limiting sail trimming. For the same reason, the sail angle remains constant when  $|\Theta_V| \in [\pi/12, \pi/4]$ .

For the simulations, we used an implementation of the full nonlinear 6-DOF model given in [10]. For these simulations, the real wind  $\vec{v}_w$  velocity is equal to  $4m/s$  and the real wind



(a) Optimal roll angle  $\phi^*$  v.s. apparent wind angle  $\Theta_V$



(b) Optimal sail angle  $\delta_s^*$  v.s. apparent wind angle  $\Theta_V$

Fig. 4: Optimal angles v.s. relative wind angle  $\Theta_V$  with limitation on  $\phi$  (with  $|V| = 5$  &  $l_\phi = 0.1$ ,  $c_1$ :  $\phi_{max} = 45^\circ$ ,  $c_2$ :  $\phi_{max} = 20^\circ$ ,  $c_3$ :  $\phi_{max} = 10^\circ$ )

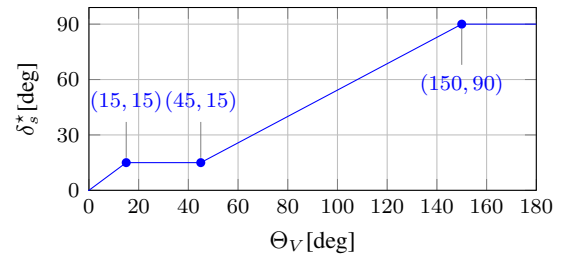


Fig. 5: Sail angle  $\delta_s$  as a function of the apparent wind angle  $\Theta_V$ , adapted from [3]

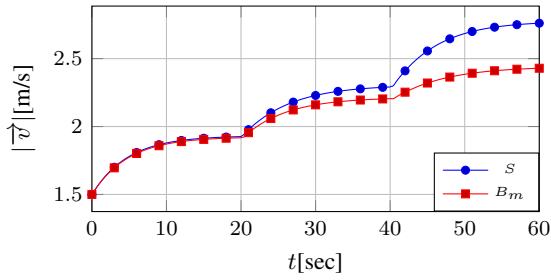
angle  $\angle v_w^B$  is a function of time as follows:

$$\angle v_w^B = \begin{cases} 10^\circ & \text{if } t \in [0, 20[ \\ 45^\circ & \text{if } t \in [20, 40[ \\ 80^\circ & \text{if } t \in [40, 60] \end{cases}$$

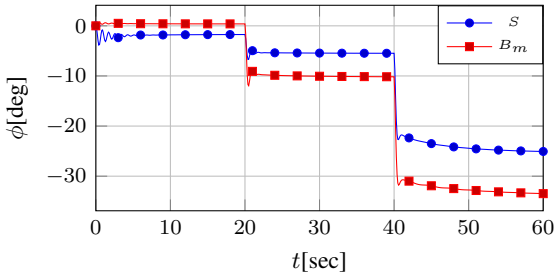
In both cases, a heading controller have been used to maintain a zero heading angle.

Simulation results (fig. 6) show that both methods perform equally when sailing downwind ( $t \in [0, 20]$ ) but the gain on velocity appears when sailing beam reach ( $t \in [20, 40]$ ) and even more when sailing upwind ( $t \in [40, 60]$ ).

Figure 7 shows the maximum velocity that can be reached by the sailboat as function of  $\angle v_w^B$  the relative angle between the heading and the true wind when  $|\vec{v}_w|$  is  $4 m/s$ . Curve  $S$  is for maximum velocity when using the presented trimming method and  $\phi_{max} = 30^\circ$  while curve  $B_m$  is for maximum velocity when trimming the sail as in 5. They



(a) Boat speed  $|v|$  over time



(b) Roll angle  $\phi$  over time

Fig. 6: Comparison between sail trimming methods ( $S$ : optimal sail angle,  $B_m$  sail trimming as in [3])

are compared with the theoretical maximum velocity ( $vel_{\max}$ ) that is obtained by simulating the system with every possible sail configuration for each wind condition. We observe that trimming the sail with  $\delta_s^*$  give better results than with [3] and that it is close to the maximum theoretical value.

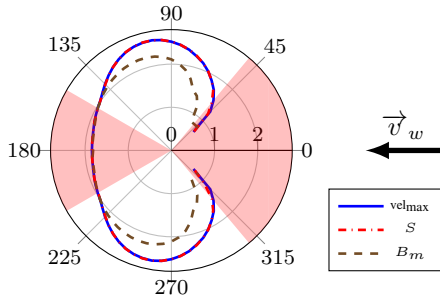


Fig. 7: Maximum velocity as function of relative angle between the followed direction and the true wind ( $S$ : optimal sail,  $B_m$  sail trimming as in [3], ( $vel_{\max}$ : maximum theoretical velocity)

## VIII. CONCLUSION

In this paper, a method was designed to optimally tune the sail angle of a sailboat in order to maximize its velocity along its current heading. This optimization takes into account a safety criterion to avoid capsizing. We show that, using this method, the heeling angle is intrinsically limited to  $\pm\pi/4$ . Moreover, other values for the maximum heeling angle (less than  $\pm\pi/4$ ) can easily be introduced in the optimization process to better reflect sailboat stability limits. As a consequence, since this optimal sail angle is computed by

studying the longitudinal force and torque generated by the apparent wind on the sail, its value depends on the apparent wind velocity, which is more consistent with the sailors practice. Numerical simulations show the performances of this method, compared to more empirical ones.

Future works will focus on designing a roll controller taking the optimal roll angle  $\phi^*$  as the reference and the sail angle  $\delta_s$  as the input to dynamically control the roll equilibrium during tacking manoeuvres for example or in case of wind gust.

## REFERENCES

- [1] G. Elkaim, "The atlantis project: A gps-guided wing-sailed autonomous catamaran," *Journal of the Institute of Navigation*, vol. 53, pp. 237–247, 2006.
- [2] M. Neal, "A hardware proof of concept of a sailing robot for ocean observation," *IEEE Journal of Oceanic Engineering*, vol. 31, no. 2, pp. 462–469, 2006.
- [3] Y. Briere, "IBOAT: An autonomous robot for long-term offshore operation," in *Electrotechnical Conference, 2008. MELECON 2008. The 14th IEEE Mediterranean*, May 2008, pp. 323–329.
- [4] N. Cruz and J. Alves, "Autonomous sailboats: An emerging technology for ocean sampling and surveillance," in *MTS/IEEE OCEANS, 2008*.
- [5] R. Stelzer, K. Jafarmadar, H. Hassler, R. Charwot, *et al.*, "A reactive approach to obstacle avoidance in autonomous sailing," in *International Robotic Sailing Conference*, 2010, pp. 33–39.
- [6] H. Erckens, G.-A. Busser, C. Pradalier, and R. Siegwart, "Avalon: Navigation strategy and trajectory following controller for an autonomous sailing vessel," *IEEE Robotics Automation Magazine*, vol. 17, no. 1, pp. 45–54, 2010.
- [7] C. Petres, M.-A. Romero-Ramirez, F. Plumet, and B. Alessandrini, "Modeling and reactive navigation of an autonomous sailboat," in *2011 IEEE/RSJ International Conference on Intelligent Robots and Systems (IROS)*, Sept. 2011, pp. 3571–3576.
- [8] L. Jaulin and F. Le Bars, "An interval approach for stability analysis: Application to sailboat robotics," *IEEE Transactions on Robotics*, vol. 29, no. 1, pp. 282–287, 2013.
- [9] R. Stelzer and T. Proll, "Autonomous sailboat navigation for short course racing," *Robotics and Autonomous Systems*, vol. 56, no. 7, pp. 604–614, 2008.
- [10] H. Saoud, M.-D. Hua, F. Plumet, and F. Ben Amar, "Modeling and control design of a robotic sailboat," in *International Robotic Sailing Conference*. Springer, 2013, pp. 95–110.
- [11] L. Xiao and J. Jouffroy, "Modeling and nonlinear heading control of sailing yachts," *IEEE Journal of Oceanic Engineering*, vol. 39, pp. 256–268, 2014.
- [12] Boehm, C., "A Velocity Prediction Procedure for Sailing Yachts with a hydrodynamic Model based on integrated fully coupled RANSE-Free-Surface Simulations," Ph.D. dissertation, Technische Universiteit Delft, 2014.
- [13] K. Legursky, "A modified model, simulation, and tests of a full-scale sailing yacht," in *Oceans, 2012*, Oct. 2012, pp. 1–7.
- [14] E. Yeh and J.-C. Bin, "Fuzzy control for self-steering of a sailboat," in *Singapore International Conference on Intelligent Control and Instrumentation, 1992. SICICI '92. Proceedings*, vol. 2, Feb. 1992, pp. 1339–1344.
- [15] R. Stelzer, T. Proll, and R. John, "Fuzzy logic control system for autonomous sailboats," in *IEEE Fuzzy Systems Conference*, July 2007, pp. 1–6.
- [16] L. Xiao, J. Alves, N. Cruz, and J. Jouffroy, "Online speed optimization for sailing yachts using extremum seeking," in *Oceans, 2012*, Oct. 2012, pp. 1–6.
- [17] K. Treichel and J. Jouffroy, "Real-time sail and heading optimization for a surface sailing vessel by extremum seeking control," in *55th International Scientific Colloquium (IWK)*, Ilmenau, Germany, 2010.
- [18] T. I. Fossen, *Handbook of Marine Craft Hydrodynamics and Motion Control*. Wiley-Blackwell, Apr. 2011.
- [19] C. A. Marchaj, *Sail Performance : Techniques to Maximize Sail Power*, 2nd ed. International Marine/Ragged Mountain Press, 2002.